Physicochemical and in Situ Photoluminescence Study of the Reversible Transformation of Oxide Ions of Low Coordination into Hydroxyl Groups upon Interaction of Water and Methanol with MgO†,||

Marie-Laurence Bailly,‡ Guylène Costentin,*,‡ Hélène Lauron-Pernot,‡ Jean Marc Krafft,‡ and Michel Che‡,§

Laboratoire de Réactivité de Surface, UMR 7609-CNRS, Université Pierre et Marie Curie, 4, place Jussieu, 75252 Paris Cédex 05, France

Received: March 19, 2004; In Final Form: June 4, 2004

The interaction of water and methanol with MgO samples with different distributions of oxide ions of low coordination has been investigated by physical techniques, particularly in situ photoluminescence. First, the three photoluminescence fingerprints of oxide ions vs their coordination number have been obtained for samples outgassed at 1273 K. By a pseudo quantitative approach, the relative distribution of the oxide ions of low coordination $O^{2-}{}_{LC}$ (where LC = 3C, 4C, and 5C refer to tri-, tetra-, and pentacoordinated oxide ions, respectively) was determined and correlated with the shape and size of MgO particles determined by TEM and XRD. The photoluminescence of surfaces of MgO obtained after outgassing at increasing temperature or after interaction of water or methanol with a clean surface, i.e., obtained by outgassing at 1273 K, was then studied and evidenced three other photoluminescent species assigned to surface OH groups. The nature and mechanism of formation of the hydroxyls groups responsible for these new luminescent species are discussed in relation with their thermal stability and FTIR experiments.

Introduction

Due to the increasing environmental pressure, development of new basic heterogeneous catalysts is an important challenge for the future. However, contrary to the case of acid catalysts, there is a lack of characterization tools to identify surface basic sites of oxides, i.e., oxide ions and hydroxyl groups and to evaluate their ability to catalyze basic reactions. In the case of alkaline earth oxides, the basicity is expected to greatly depend on the distribution of oxide ions of low coordination (LC) $O^{2-}{}_{LC}$, and on the hydroxyl coverage of the surface.[1,2] Photoluminescence spectroscopy is one of the very few techniques able to discriminate oxide ions as a function of their coordination number.[2,3] It probes the surface of the solid via a ligand to metal charge transfer: $Mg^{2+}O^{2-} + h\nu \rightarrow Mg^{+}O^{-}$. Indeed, according to Tench and Pott[4] and Zecchina et al.,[5−7] well-outgassed high surface area MgO powders exhibit abnormal absorption at much lower energy than the band gap of the corresponding bulk oxide. The values correlate with the surface band gap calculated from the expression of Levine and Mark[8] for different surface planes of MgO. Recent theoretical studies[9] confirm that photoluminescence is particularly sensitive to the coordination of the O^{2-} ions. To use this technique to evaluate the basicity of a surface, the nature of the luminescent species formed by interaction of $O^{2-}{}_{LC}$ with a protic molecule has to be investigated.

In a previous study,[10] we have shown that technical improvement of the photoluminescence cell and its coupling to a dynamic vacuum system result in spectra of MgO better resolved and more stable in time. A pseudo quantitative approach was also developed to determine the relative distribution of $O^{2-}{}_{LC}$ ions.

The purpose of this paper is to investigate by physical techniques, particularly in situ photoluminescence spectroscopy, the interaction of oxide ions of a MgO surface toward water or methanol as a function of their coordination number.

Usually, the preparation of oxides with different distributions of $O^{2-}{}_{LC}$ ions is achieved by outgassing samples at increasing temperature to desorb contaminants, and thus to the progressive recovery of surface $O^{2-}{}_{LC}$. However, the presence of remaining adsorbates in the vicinity of the already liberated oxide ions cannot be avoided using such procedure. Our approach consists of the preparation of MgO samples with different morphologies by varying the experimental conditions as well as the subsequent thermal treatments: the proportions of oxide ions at terraces, edges or corners namely $O^{2-}{}_{5C}$, $O^{2-}{}_{4C}$, and $O^{2-}{}_{3C}$ ions respectively are different from one sample to another, on clean surfaces (free from any carbonates or hydroxyls groups).

These samples are characterized principally by in situ photoluminescence and a pseudo quantitative approach is established to estimate the relative distribution of populations of $O^{2-}{}_{LC}$.

Peculiar attention is given to the complete identification of luminescent species with systematic determination of both excitation and emission wavelengths. The interaction with water is studied on high surface area samples either by thermal desorbing or upon adsorption of water on a high-temperature pretreated sample. The effect of the presence of hydroxyls groups on photoluminescence signal is thus described. The nature of the hydroxyls groups responsible for these new luminescent species is discussed in relation with their thermal stability, the results of methanol adsorption and FTIR experi-

† Part of the special issue "Michel Boudart Festschrift".

|| A part of this paper was recently presented as an oral communication at 13ICC, Paris, July 11−16, 2004.

* To whom correspondence should be addressed. E-mail: costenti@ccr.jussieu.fr.

‡ Laboratoire de Réactivité de Surface, UMR 7609-CNRS, Université Pierre et Marie Curie.

§ Institut Universitaire de France.

10.1021/jp048760+ CCC: $30.25
Published on Web 08/17/2004

ments. In fact, even if the identification by FTIR of the local structure of OH groups on MgO is still under debate:[11−14] it is however generally admitted that distinction should be made between "isolated" OH groups (narrow band at 3740 cm^{-1}) and "linked" OH groups (involved in hydrogen bonding) (around 3650 cm^{-1}).

Experimental Section

Sample Preparation. MgO samples were prepared starting from two kinds of precursors, magnesium hydroxide or metallic magnesium.

−MgO-ex-hydroxide was prepared by thermal decomposition of three $Mg(OH)_2$ brucite precursors prepared as follows:

(i) $Mg(OH)_2$-hydration was obtained by stirring a commercial MgO (Aldrich, 99,99%) in water for 24 h at room temperature (rt). The resulting product was dried in primary vacuum at 373 K for 3 h.

(ii) $Mg(OH)_2$-precipitation was obtained from $Mg(NO_3)_2$ (Aldrich, 99,99%) solution using ammonium hydroxide (Aldrich, 99%) (8 M) as precipitating agent. Thus, the latter was added to a magnesium nitrate solution (1 M) and the pH value adjusted to 10 at 303 K. After stirring for 30 min, the precipitate was washed several times with deionized water, then filtered and finally dried at 333 K in primary vacuum for 3 h.

(iii) $Mg(OH)_2$-sol−gel was obtained by hydrolysis of magnesium methanolate, $Mg(OCH_3)_2$. Absolute methanol (75 mL) was added to 4 g of Mg powder previously dried at 353 K in primary vacuum for 30 min. The mixture was then stirred and heated under reflux for 20 h. A few drops of water were added to the mixture and the resulting gel was dried at 313 K in primary vacuum for 3 h. Note in this case that as observed by XRD, some of the OH groups of this $Mg(OH)_2$ phase are replaced by methoxy groups, as reported earlier.[15] The latter were eliminated by treatment of the sample under 100 Torr of oxygen at 673 K for 30 min.

All the hydroxide samples were finally treated in a vacuum (10^{-6} Torr) up to 1273 K (ramp 1 $K.min^{-1}$) and maintained at this temperature for 2 h. This final treatment was chosen because it gave reproducible results. It resulted in samples hereafter referred to as MgO-hydration, MgO-precipitation and MgO-sol−gel, respectively.

−MgO ex-metallic magnesium were prepared by direct oxidation of the metal:

(i) MgO-smoke was prepared by burning Mg ribbons (Aldrich, 98%) in static air above the melting temperature, 923 K, and collecting the resulting oxide on silica plates.[16]

(ii) MgO−CVD was obtained by chemical vapor deposition as described earlier.[17,18] Metallic magnesium vapor was oxidized by O_2/Ar in a flow reactor system.

Characterization Techniques.

Structure and Morphology. X-ray powder diffractograms were recorded with a Siemens diffractometer. The instrument was equipped with a copper anode generator CuKα (λ = 1.5418 Å). Diffractograms were recorded in the 2θ range 10 to 60°.

Specific surface areas were measured by adsorption of N_2 on a Micromeritics apparatus and calculated according to the BET method.

For TEM characterizations, the MgO powder was suspended in ethanol and then rapidly supported on a copper grid. All observations were made with a JEOL JEM 100 CXII UHV using a 100 keV electron beam.

Molecular Level Characterization. For FTIR studies, samples were used as self-supported wafers of about 10 mg. Decarbonatation and dehydroxylation of the samples were followed versus pretreatment temperature. All spectra were registered at room temperature using a Nicolet FTIR-710 spectrometer, after outgassing the sample.

***In situ* Photoluminescence Experiments.**

Procedure. The photoluminescent cell, described in a previous paper,[10] was connected to a vacuum system, that allowed both thermal pretreatments and adsorption−desorption experiments to be performed in situ. Samples were outgassed (ramp 1 $K.min^{-1}$) up to 1273 K and kept at this temperature for 2 h under dynamic vacuum to a final pressure of 10^{-6} Torr to remove both carbonates and hydroxyls groups, as shown below. The resulting surface of such samples will hereafter be referred to as clean surface.

The effects of the interaction of water or methanol with MgO were studied by introducing the gases via the vacuum line connected to the spectrometer. Distilled water and methanol (Prolabo, RP Normapur) were previously purified by the freeze−pump−thaw technique. Adsorption of water and methanol was carried out at 373 K and room temperature respectively. Successive doses were introduced until the equilibrium pressure reached 1 Torr (1 Torr = 133.32 Pa). After 15 min of contact, the sample was outgassed at room temperature and then heated by steps of 100 K from 273 to 673 K, the cell being isolated: this thermal treatment will hereafter be referred to as the activation procedure. The sample was then progressively heated to 1273 K under vacuum and maintained at this temperature until a 10^{-6} Torr pressure was reached: this thermal treatment will hereafter be referred to as the evacuation procedure. All the spectra were registered at room temperature after evacuation (10^{-6} Torr).

Spectra Recording. The photoluminescence spectra were recorded at room temperature under dynamic vacuum, using a spectrofluorophotometer Spex Fluorolog II from Jobin-Yvon (equipped with 450W Xe lamp as excitation source, and color filters to eliminate scattered light). The excitation wavelengths were selected using a double monochromator. Due to the energy range of the source, only excitation wavelengths above 220 nm were available. The excitation and emission band-passes were 5 and 1.9 nm, respectively, for all the results reported here.

Data Processing. For the determination of the fingerprints of photoluminescent species, systematic identification of the couples of excitation−emission wavelengths was performed, by optimizing the photoluminescent yields (number of photons emitted from the excited state to the number of photons absorbed by the ground-state molecule):[3] a photoluminescent center is believed to be correctly identified by its couple (λ_{exc}−λ_{em}), if the intensity of the excitation band fits that of the corresponding emission band.[3]

Decomposition of the spectra in their several components was made with ORIGIN 6.1 from OriginLab Corporation, using Gaussian curves.

Results and Discussion

X-ray Diffraction and BET Measurements. The X-ray powder diffraction patterns show that the hydroxide precursors have the $Mg(OH)_2$ brucite structure (JCPDS 7-0239). All the MgO samples exhibit the typical periclase structure (JCPDS 4-0239). From the width of the (100) peak, the average particle size was estimated. From the results summarized in Table 1, no direct correlation between surface area and particle size could be evidenced.

Transmission Electron Microscopy. Both MgO-precipitation (Figure 1b) and MgO-sol−gel (Figure 1c) exhibit the particle shape usually described for $Mg(OH)_2$ brucite precursors,

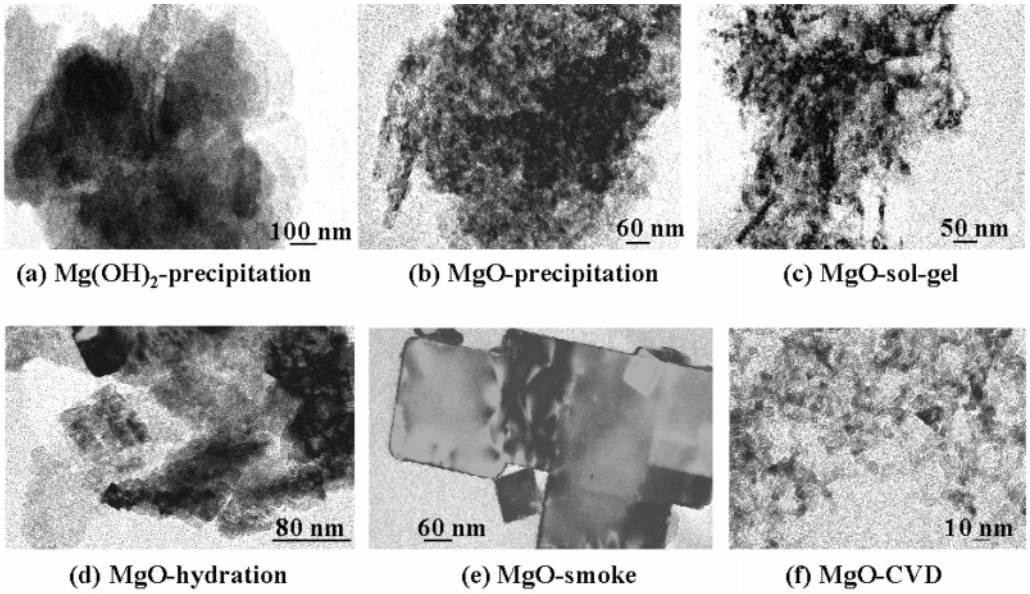

Figure 1. TEM pictures of (a) $Mg(OH)_2$-precipitation, (b) MgO-precipitation, (c) MgO-sol−gel, (d) MgO-hydration, (e) MgO-smoke, and (f) MgO−CVD.

TABLE 1: Specific Surface Area and Particle Size of the Different MgO Samples

sample	specific surface area (m^2g^{-1})	particle size (XRD) (Å)
MgO-smoke	10	450
MgO-hydration	168	180
MgO−CVD	300	70
MgO-precipitation	198	75
MgO-sol−gel	150	87

i.e., large hexagonal plates, (Figure 1a).[19,20] Starting from these hexagonal particles, and upon thermal treatment, highly irregular surfaces indicating steep stairs with successions of steps and small terraces are obtained. According to literature data,[21,22] the departure of water molecules formed from hydroxyl groups of the brucite lattice and the resulting growth of MgO periclase nuclei lead to constraints and breaking of the layers of the precursor hydroxide structure. Consequently, the high concentrations of edges and corners observed are characteristic features of the two MgO-ex-hydroxide samples, in relation with their formation mechanism. This effect is even more pronounced in case of MgO-sol−gel, because of additive defects induced by the departure of remaining methoxy groups: the TEM picture (Figure 1c) shows even more ill-defined particles.

By contrast,$Mg(OH)_2$-hydration does not involve such hexagonal plate morphology (not shown). In fact, the particles shape is closer to that of its cubic precursor (commercial MgO), with periclase structure. As a result, MgO-hydration involves particles which are larger than for MgO-precipitation and MgO-sol−gel samples, and which are organized as agglomerates of cubes (Figure 1d).

MgO-smoke (Figure 1e) and MgO-CVD (Figure 1f) show cubic particles with edge lengths mostly around 450 and 70 Å, respectively. Rounded corners observed on some of the particles of MgO-smoke sample can be assigned to a early stage erosion well-known for this system.[16]

In relation with the preparation modes, and on the basis of their morphology, the MgO samples can be classified into two groups: (i) MgO-smoke, MgO-CVD, and MgO-hydration with cubic particles exposing large (100) planes with mainly $O^{2-}{}_{5C}$ ions, and, (ii) MgO-precipitation and MgO-sol−gel for which the proportion of ions in lower coordination ($O^{2-}{}_{4C}$, $O^{2-}{}_{3C}$) is expected to be larger.

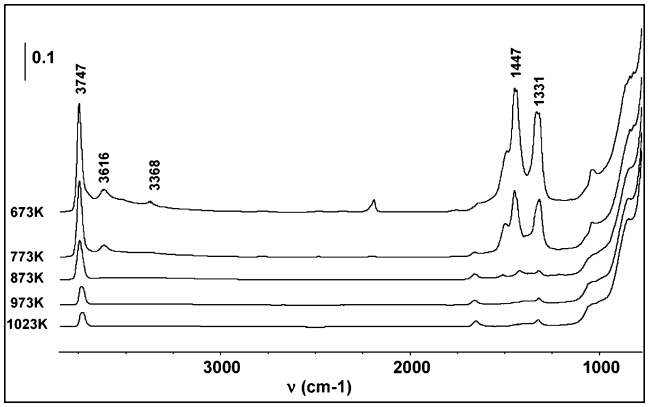

Figure 2. FTIR spectra of the carbonate and OH regions versus pretreatment temperature of $Mg(OH)_2$-hydration.

Infrared Spectroscopy. The removal of surface carbonates and hydroxyls of $Mg(OH)_2$-hydration was studied using FTIR as a function of the outgassing temperature (Figure 2). The 1300−1500 cm^{-1} bands associated with carbonates on MgO[23] decrease in intensity and become weak from 873 K. The 3600−3780 cm^{-1} region reveals two kinds of OH bands: a broad band around 3600−3650 cm^{-1} relative to "associated" OH, i.e., interacting by hydrogen bonding and a quite narrow band around 3700−3750 cm^{-1}, assigned to "isolated" hydroxyl groups.[11,12,24] By increasing the outgassing temperature, the two bands decrease in intensity, but the broad band around 3600 cm^{-1} is no longer visible at 873 K whereas that at 3740 cm^{-1} still remains up to 1023 K (Figure 2), which is the maximum temperature attainable with our FTIR experimental setup. Outgassing the samples at 1273 K removes most carbonates and hydroxyl groups, as confirmed below by photoluminescence.

Photoluminescence.

I. Evidence for Oxide Ions of Low Coordination. (a) Probing Three Luminescent Centers. Two samples, MgO-sol−gel and MgO-smoke representative of each group of samples previously described are now studied. Figure 3 gives the emission spectra of these samples excited at high energy (230 nm) which mainly consist of a broad band around 380 nm. The corresponding

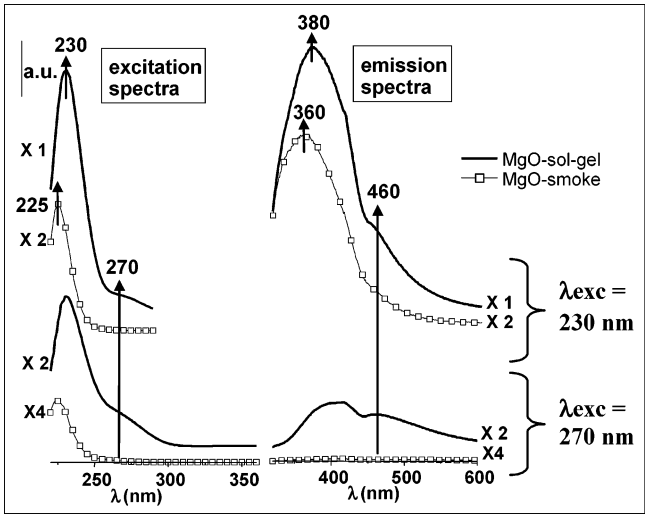

Figure 3. Emission spectra monitored at 230 and 270 nm of the clean MgO-sol−gel (—) and MgO-smoke (□) and corresponding excitation spectra monitored at the maximum of emission.

excitation spectra recorded at maximum of emission are also reported. Apart from the lower intensity of the emission band observed for MgO-smoke, consistent with its lower surface area (Table 1), the similarity of the intensities of the emission and excitation bands for each sample allows to identify a first kind of photoluminescent species, excited at 230 nm, and emitting at around 380 nm, hereafter noted as (230−380).

The two MgO-sol−gel and MgO-smoke samples differ in the following aspects:

−MgO-sol−gel exhibits an excitation band involving a shoulder at around 270 nm, absent for MgO-smoke. A specific excitation at 270 nm leads to the emission spectra reported on Figure 3. It clearly evidences an emission band at 460 nm, which only appears as a shoulder on the emission spectrum monitored at 230 nm. The excitation spectrum corresponding to the emission at 460 nm was then recorded: the intensity of the shoulder at 270 nm is similar to the one of the emission band at 460 nm monitored with an excitation at 270 nm suggesting the existence of a second kind of photoluminescent species excited at 270 nm and emitting at 460 nm, hereafter noted as (270−460). The corresponding curves for MgO-smoke do not show evidence for such kind of photoluminescent species.

−The positions of maximum intensity (λ_{max}) of the emission spectra are slightly different (380 and 360 nm for MgO-sol−gel and MgO-smoke respectively), whereas those of the excitation spectra are closer (230 and 225 nm, respectively), suggesting the existence of another photoluminescent center present in different proportions in the two samples. The contribution of this center is occurring at higher energy (lower wavelength) and the corresponding band cannot be resolved from the contribution of the first kind of species (230−380). The maximum emission of this third photoluminescent center excited at higher energy, hereafter noted as (<220 − < 350) cannot be determined because of the limited energy of the Xe UV−visible source of the spectrometer.

(b) Band Assignments. The pretreatment of all the samples at 1273 K (ramp 1 $Kmin^{-1}$) for 2 h under dynamic vacuum removes the remaining carbonates or hydroxyl groups to leave only bare $Mg^{2+}{}_{LC}O^{2-}{}_{LC}$ pairs. On the basis of our data and taking into account (i) the different morphologies of MgO-sol−gel and MgO-smoke described earlier, (ii) the high thermal outgassing of the samples, and (iii) the variation of the Madelung potential with the coordination number,[25] the (270−460) and (230−380) luminescent species can be associated to $O^{2-}{}_{3C}$ and $O^{2-}{}_{4C}$ ions, respectively. The $O^{2-}{}_{5C}$ ions also give a photoluminescence contribution at lowest wavelength, around 350 nm, which is not well resolved from the $O^{2-}{}_{4C}$ emission. The convolution of the two contributions leads to a broadening and displacement of the maximum of the band.

TABLE 2: Particle Morphology, $\lambda_{em\ max}$ and $O^{2-}{}_{3C}/O^{2-}{}_{4C}$ Ratio for the Different MgO Samples

sample	particles morphology	$\lambda_{em\ max}$ (nm) (λ_{exc} = 230 nm)	$O^{2-}{}_{3C}/O^{2-}{}_{4C}$
MgO-smoke	cubes	360	≈0
MgO-hydration	cubes	375	0.012
MgO−CVD	cubes	370	0.05
MgO-precipitation	irregular particles	380	0.06
MgO-sol−gel	irregular particles	380	0.15

The implication of F centers in the photoluminescence of MgO was also reported,[26,27] but the corresponding band appears at lower energy than that observed for our samples. Our assignments of excitation bands to $O^{2-}{}_{LC}$ sites are supported by UV−vis diffuse reflectance experiments reported by Garrone et al.[25] Moreover, on the basis of theoretical studies, Shluger et al.[9] concluded that there is a strong dependence of the spectroscopic properties on coordination. Previous experimental photoluminescence studies on MgO[16,28] underlined the dependence of the photoluminescence properties on sample preparation and treatment with different gases in line with our data concerning the excitation values. However, if Coluccia et al.[16] assigned the excitation at 230 and 270 nm to $O^{2-}{}_{4C}$ and $O^{2-}{}_{3C}$ respectively, the lack of resolution of the emission spectra led to a broad emission band centered around 400 nm. It should also be noted that, according to Anpo et al.,[28] the 270 nm excitation associated with the emission at 420 nm was assigned to hydroxyl groups.

(c) Distribution of the Populations of Oxide Ions of Low Coordination. All of the MgO samples characterized following the same approach exhibit the same three kinds of species, but in different ratios. A pseudo quantitative approach has been developed[10] which is based on the analysis of deconvoluted excitation spectra registered at room temperature. The $O^{2-}{}_{3C}/O^{2-}{}_{4C}$ ratio obtained from the ratio of the areas of the deconvoluted excitation peaks at 270 and 230 nm monitored at 460 and 380 nm, respectively, and the values at maximum of emission, $\lambda_{em\ max}$, for the different MgO samples are summarized in Table 2.

As expected, among the first series of samples (MgO-smoke, MgO-CVD, and MgO-hydration with cubic particles), the concentration of corners depends on the particle size (Table 1): the larger the particles, the lower the $O^{2-}{}_{3C}/O^{2-}{}_{4C}$ ratio. Moreover, the shift of $\lambda_{em\ max}$ toward higher energy (Table 2) depends on the amount of $O^{2-}{}_{5C}$: the more important the contribution of the $O^{2-}{}_{5C}$ species in the emission spectra, the larger the shift of the broad line toward lower wavelength.

The second series of samples (MgO-sol−gel and MgO-precipitation) whose morphology arises from the changes of the hexagonal plates upon dehydroxylation, involves particles with the lowest $O^{2-}{}_{5C}$ abundance, and thus the highest $\lambda_{em\ max}$ value. It is noteworthy to underline that, compared to MgO-precipitation and despite comparable particle size and lower specific surface area, MgO-sol−gel has a larger concentration of $O^{2-}{}_{3C}$ ions. It can be proposed that the decomposition of its brucite precursor which exhibits few methoxy groups[15] leads to a more defective MgO.

These results clearly confirm that the distribution of populations of oxide ions of low coordination depends on preparation

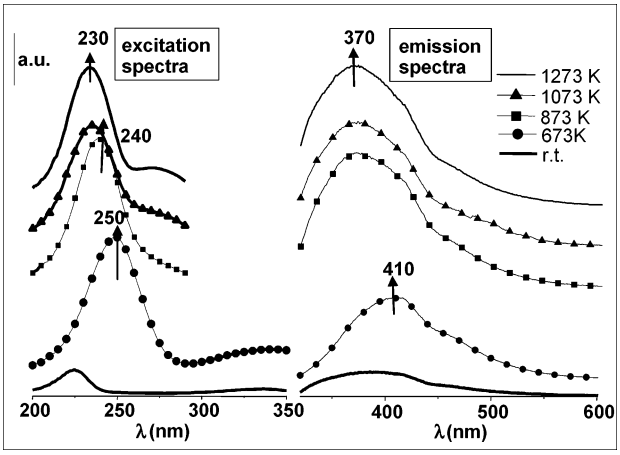

Figure 4. Emission spectra monitored at 230 nm of MgO−CVD outgassed at increasing temperature and corresponding excitation spectra monitored at the maximum of emission.

method. However, a refined estimation of $O^{2-}{}_{3C}/O^{2-}{}_{4C}$ ratio will be performed considering low-temperature spectra to limit the energy transfer phenomenon.[29−31]

II. Evidence for Surface OH Groups. In the following sections, the effect of (de)hydroxylation on the photoluminescence of the samples is studied, taking into account the emission spectra monitored with excitation at 230 nm. The modification of the nature of the surface sites is systematically checked by recording the corresponding excitation spectra. When significant shifts of λ_{exc} values relative to those characteristic of the three kind of species already evidenced on the clean surface are observed, new emission spectra are monitored with the correct excitation wavelengths to determine the ($\lambda_{exc}-\lambda_{em}$) couple relative to the new luminescent species.

(a) Effect of Outgassing Temperature on the Photoluminescence Properties of MgO-CVD. First, the photoluminescence response of MgO surface outgassed at increasing temperature is followed. This procedure, which is supposed to progressively eliminate the quenching due to oxygen and to clean the surface from possible contamination by water or any other air contaminant, results in the recovering of photoluminescence bands characteristic of clean MgO surface. In fact, Anpo et al.[28] reported from the analysis of the gases evolved during outgassing, that the major component was H_2O, mainly in the 673−873 K range, with CO_2 in minor amount. Outgassing the sample above this temperature leads to the desorption of only a small amount of water.

Only the results concerning the sample involving the highest specific surface area, MgO-CVD, are reported here because they are representative of the other samples.

(i) Excitation at 230 nm. The emission spectrum monitored with excitation at 230 nm (Figure 4) and recorded after outgassing at room temperature differs from that of the corresponding clean MgO (similar to that shown on Figure 3): it exhibits very weak and broad bands suggesting that adsorbates on the surface are present and at the origin of this low intensity. The recovering of the characteristic MgO spectrum is achieved by outgassing the sample at increasing temperature. However, Figure 4 shows that, upon increasing the outgassing temperature, the emission spectrum drastically changes, not only in intensity but also in shape, with a shift of the $\lambda_{em\ max}$ value to high energy suggesting a modification of the nature of the photoluminescent species upon outgassing.

In the range rt-673 K, the intensity of the band increases with the outgassing temperature with a maximum of emission at 410 nm relative to the excitation at 250 nm. The discrepancy between the intensities of the emission and excitation bands is due to the fact that, monitoring the emission spectrum at 230 nm does no longer correspond to an optimization of the yield of the emission. This result suggests that the species excited at 250 nm and emitting at 410 nm are different from those described for the clean MgO surface. From the excitation spectra, it can be seen that there are other contributions excited in the 300−370 nm range which are not well resolved.

After outgassing at 873 K, MgO-CVD excited at 230 nm exhibits an emission very similar to that of the clean MgO. However, the excitation spectrum of the sample outgassed at 873 K exhibits a maximum at 240 nm, not at 230 nm the characteristic excitation wavelength of $O^{2-}{}_{4C}$ ions. It can thus be concluded that the adsorbates responsible for the quenching of the excitation due to $O^{2-}{}_{4C}$ ions start to be eliminated to form CO_2 and water.

When MgO-CVD is outgassed at 1273 K, the intensities of the bands do not really increase, whereas the shift of the excitation wavelength from 240 to 230 nm indicates that, above this temperature, the excited species are oxide ions only. Indeed, the excitation spectra are typically characteristic of the clean MgO surface with a first band at 230 nm due to $O^{2-}{}_{4C}$, and a second at 270 nm due to $O^{2-}{}_{3C}$, both kinds of species being still covered by protons when the pretreatment is performed below 1073 K. Taking into account the temperatures of departure of CO_2 and water,[28] these results confirm that the removal of OH groups to form H_2O is closely associated with the appearance of photoluminescence characteristic of oxide ions.

(ii) Other Excitations. To better characterize the photoluminescent species evidenced for samples outgassed below 1273 K, their specific excitation has to be precisely identified. On the basis of the results deduced from the excitation spectra given in Figure 4, an emission spectrum of MgO-CVD is then monitored at 250nm (Figure 5a). The similarity of the intensities of its maximum at 410 nm and of the corresponding excitation band obtained for an emission at 410 nm allows to identify an additional kind of photoluminescent species, hereafter noted as (250−410). In the same manner, emission spectra monitored at 350 nm of MgO-CVD outgassed at increasing temperature are reported on Figure 5b. The sample outgassed at room temperature exhibits weak bands (not shown) probably because of quenching phenomena due to adsorbates. The intensities increase upon outgassing the sample at 673 K. Excitation at 350 nm leads to an emission spectrum with two maxima, at 410 and 470 nm whose corresponding excitation contributions are found at 350 and 370 nm, respectively. Thus, two other photoluminescent species excited at 350 and 370 nm can be identified with emissions at 410 and 470 nm respectively and hereafter noted as: (350−410) and (370−470).

MgO-CVD outgassed at 873 K does no longer exhibit emission when excited either at 370 or at 350 nm. The disappearance of the (350−410) and (370−470) species is confirmed by the excitation spectra monitored with emission at 410 and 470 nm. However, the (250−410) species still remain, and a shoulder at 280 nm also appears, as shown by excitation spectra on Figure 5b. The latter cannot be related to the recovering of the $O^{2-}{}_{3C}$ ions as there is no emission at 460 nm. The corresponding emission is difficult to identify because of the contribution of the (250−410) species. From examination of spectra reported on Figure 4, it seems that $O^{2-}{}_{4C}$ starts to be released above 873 K (the associated emission signal at 370 nm is recovered and the excitation band shifts above this

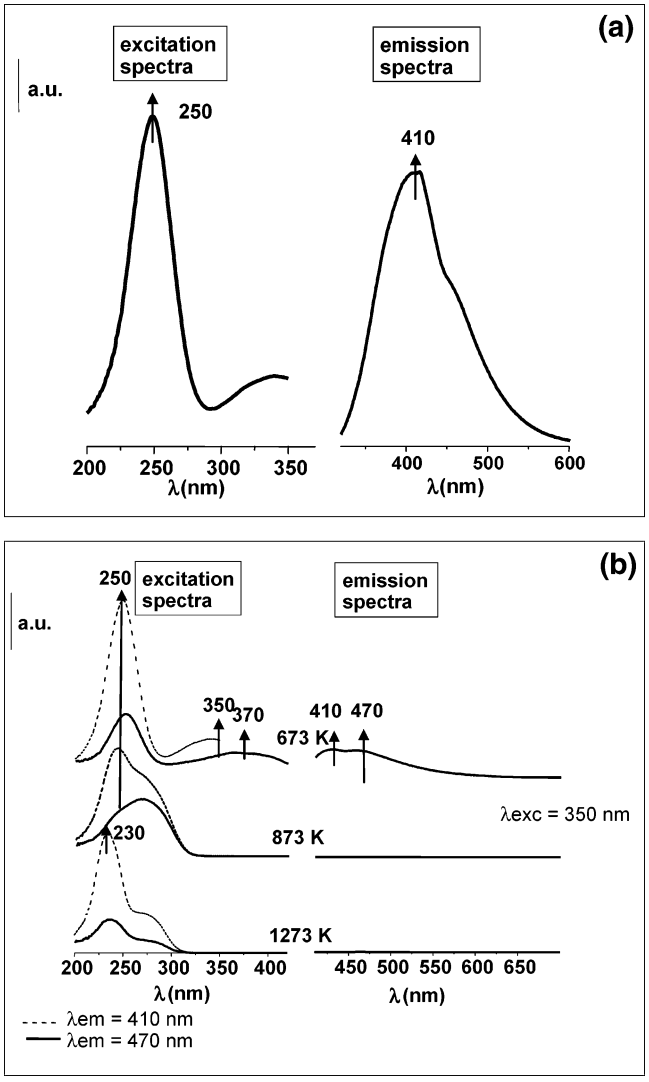

Figure 5. (a) Emission spectrum monitored at 250 nm of MgO−CVD outgassed at 673 K and corresponding excitation spectrum. (b) Emission spectra monitored at 350 nm of MgO−CVD outgassed at increasing temperature and corresponding excitation spectra monitored at the two maxima of the emission bands (410 and 470 nm).

temperature), in relation with the deprotonation of the corresponding $O_{4C}H^-$.

After outgassing at 1273 K, the three species above are no longer observed in contrast to the species [(<220 − < 350), (230−380), and (270−460)] typical of the clean surface which all are recovered (Figure 4).

The fingerprints of the different photoluminescent species observed on MgO are gathered in Table 3. Due to the broadness of the emission bands, further investigations including time-resolved spectroscopy will be performed to confirm the number of the various photoluminescent contributions to be considered.

(b) Interaction of Water with MgO-sol−gel. In connection with these results, the effect of the adsorption/desorption of H_2O on the photoluminescence spectra of MgO, already considered by Coluccia et al. on MgO ex carbonate samples,[32] has been reinvestigated on samples previously outgassed at 1273 K. This temperature was chosen so as to ensure that the modifications of the photoluminescence properties could be due only to hydroxyl groups and/or water. Because it was found that the surface of MgO-CVD is reconstructed upon water interaction,[33] in a similar way to that which was earlier described for MgO-smoke,[16,34] MgO-sol−gel was chosen for this study. Indeed, it has been checked that this sample is not modified upon hydroxylation.

TABLE 3: Photoluminescence Characteristics of Species Observed on MgO

λ_{exc} (nm)	λ_{em} (nm)	Assignment
< 220	< 350	O^{2-}_{5C}
230	380	O^{2-}_{4C}
270	460	O^{2-}_{3C}
250	410	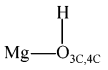
350	410	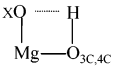
370	470	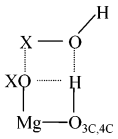

X=H, CH_3.

(i) Adsorption. Water vapor increments (0.4 to 1 μmol) progressively introduced in the sample cell lead to a decrease of intensity of the photoluminescence monitored for excitation at 230 nm (Figure 6a). Since the sample is outgassed before recording the spectra, the quenching phenomenon is related to molecules strongly adsorbed at the surface. Moreover, the intensities of the contributions relative to O^{2-}_{4C} and O^{2-}_{3C} decrease in parallel showing no selectivity of water interaction toward the coordination of oxide ions.

After the equilibrium pressure has reached 1 Torr, and subsequent outgassing, the emission monitored for excitation at 230 nm and the corresponding excitation spectra are almost totally quenched. Concomitantly, the two contributions relative to (350−410) and (370−470) species clearly grow (Figure 6b). These results confirm that these two species already described in section II (a) are definitely related to hydroxyl ions. It should be underlined that the (250−410) species are not observed.

(ii) Activation. After adsorption of water, MgO-sol−gel is heated stepwise from 373 to 673 K, in a closed cell, then cooled to room temperature and finally outgassed until a pressure of 10^{-6} Torr is reached. An important increase of intensity of both components relative to (350−410) and (370−470) species is observed from 373 to 573 K on spectra reported on Figure 6b. Moreover, the (250−410) species are formed from 573 K. Concomitantly, a new kind of species excited at 310 nm is formed, whose corresponding emission cannot be unambiguously determined. Both species are clearly visible from 573 K and their contributions still increase at 673 K. These features cannot result from the progressive decrease of quenching phenomena following the desorption of adsorbates. As a matter of fact (i) during this procedure, the final outgassing is performed only once the sample has been cooled to room temperature: the possible desorption of molecules participating to quenching upon heating would have been reversible upon cooling, (ii) the intensities of emission spectra monitored at 230

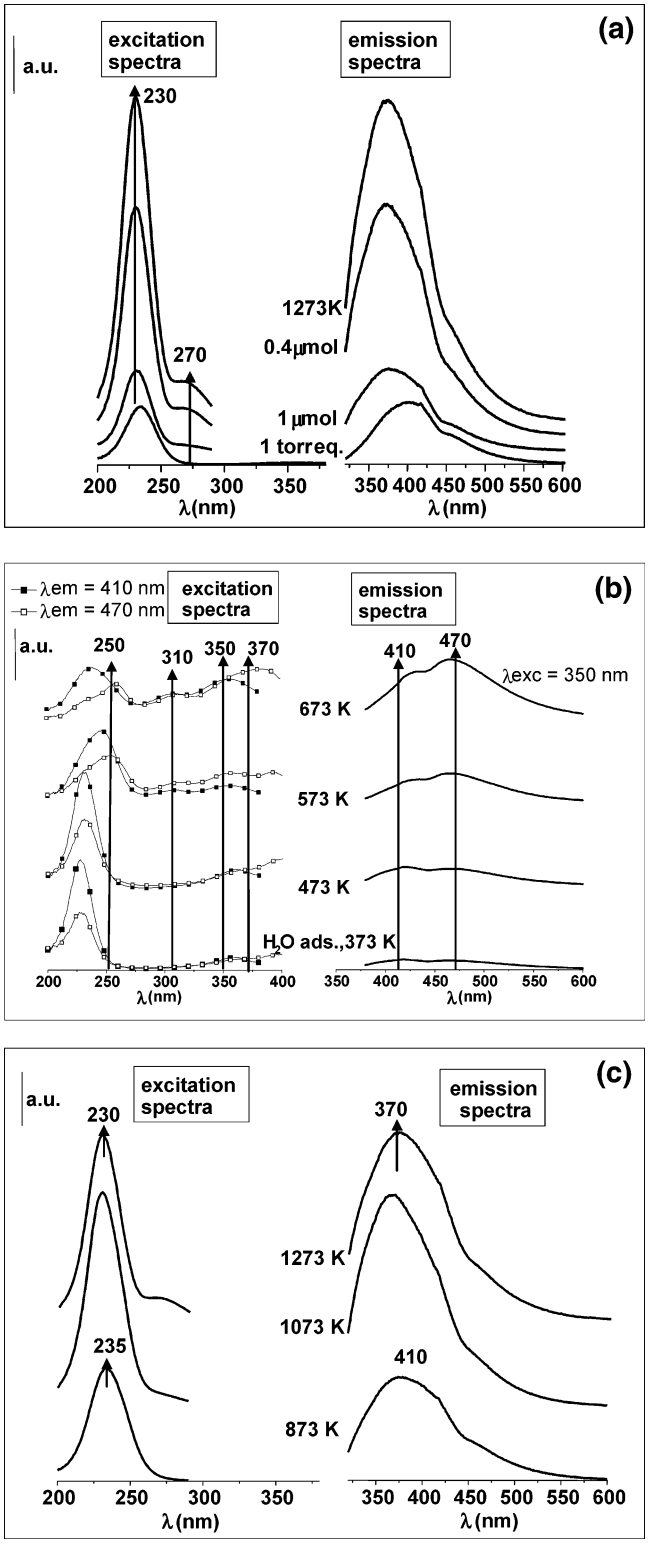

Figure 6. MgO-sol−gel previously outgassed at 1273 K (a) Emission spectra monitored at 230 nm and corresponding excitation spectra monitored at the maximum of emission after introduction of increasing dose of water, (b) Emission spectra monitored at 350 nm and corresponding excitation spectra monitored at the maxima of the emission bands (410 and 470 nm) after introduction of an equilibrium pressure of water of 1 Torr and subsequent activation at increasing temperature (c) Emission spectra monitored at 230 nm and corresponding excitation spectra monitored at the maximum of emission during evacuation procedure at increasing temperature.

nm (not shown) do not increase in parallel. Indeed, from the emission spectra monitored at 250 and 230 nm and the

SCHEME 1: Representation of the Different Kinds of OH Groups Formed upon Water or Methanol Dissociative Adsorption

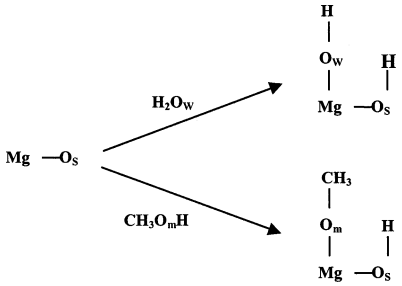

corresponding excitation spectra, it appears that the $O^{2-}{}_{4C}$ species still present at 473 K are no longer observed at 573 K.

It can thus be concluded, that water dissociation is activated by heating with an increase of photoluminescent species relative to OH groups at the expense of that relative to bare oxide ions. Thus, both dissociative and molecular adsorption of water on the surface of MgO must be considered.

(iii) Evacuation. MgO-sol−gel is outgassed at higher temperature and cooled to room temperature before spectra recording. For the sample outgassed at 873 K, species (350−410), (370−470) and that excited at 310 nm disappear to the benefit of species (230−380), i.e., $O^{2-}{}_{4C}$ ions (Figure 6c). The excitation band exhibits a maximum at 235 nm due to remaining contribution of the (250−410) species. Species $O^{2-}{}_{3C}$ still covered by protons at this outgassing temperature start to be released after outgassing at 1073 K. Comparison of the sample outgassed at 1273 K before and after water treatment indicates that the transformation observed upon interaction of the clean surface with water is completely reversible.

(c) Interaction of Methanol with MgO-sol−gel. The adsorption−desorption procedure for methanol was the same as for water. Assuming dissociative adsorption of the former, only O_s−H hydroxyls (O_s is a lattice surface oxide ion) are expected to form,[35−38] whereas, for water, Mg−O_w−H hydroxyls (O_w coming from water molecule) also form, as represented on Scheme 1.

Idriss et Barteau[39] reported that adsorption of formic acid or methanol on ZnO led to an increase of photoluminescence, due to the formation of new luminescent species upon dissociative adsorption.

Adsorption of methanol is carried out on MgO-sol−gel outgassed at 1273 K. Globally, the same phenomena already described upon water adsorption are observed: the interaction with methanol first quenches the signal relative to the bare surface; concomitantly photoluminescent species appear in the 420−470 region, whose contributions grow during the activation procedure. The subsequent evacuation progressively leads to the reverse transformation: decrease of these photoluminescent species at the benefit of progressive recovery of $O^{2-}{}_{5C}$, $O^{2-}{}_{4C}$, and $O^{2-}{}_{3C}$ ions.

The crucial point is to compare the nature of the photoluminescent species observed here with the three species reported in the case of water adsorption (Table 3). Figure 7a reports the emission and the corresponding excitation spectra for MgO-sol−gel once an equilibrium pressure of methanol of 1 Torr has been reached and after activation at 573 K: emissions at 410 and 470 nm are associated with excitation at 250 and 350 nm respectively on one hand, and at 370 nm on the other hand. The main result is that the species observed here exhibit the same fingerprints as the ones observed for water adsorption. Moreover, from the comparison of the intensities of the signals

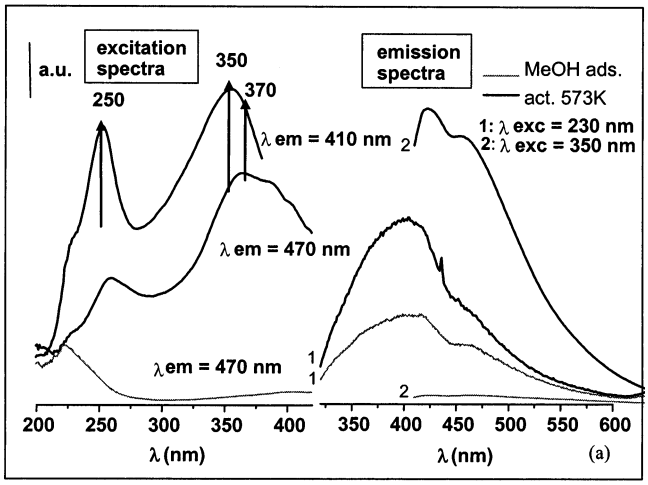

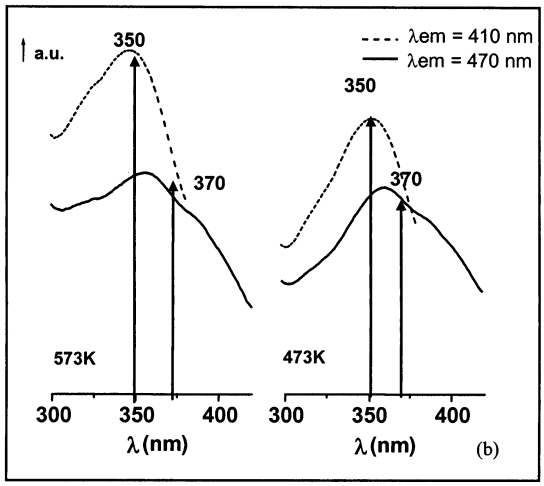

Figure 7. (a) Emission spectrum monitored at 230 and 350 nm of MgO-sol−gel and corresponding excitation spectra monitored at the two maxima of emission bands (410 and 470 nm) after introduction of an equilibrium pressure of methanol of 1 Torr at room temperature followed by activation at 573 K. (b) Comparison of the excitation spectra monitored at 410 and 470 nm after activation procedure at 473 and 573 K.

relative to (350−410) and (370−470) species, it appears that the (370,470) species grows less rapidly than that of the (350−410) species during activation procedure (Figure 7b). The weak excitation bands at 280 and 310 nm already observed in sections IIa and IIb, respectively, cannot be excluded here.

(d) Assignment of the Photoluminescence Bands Observed on an Hydroxylated Surface. Both outgassing and hydration of MgO surfaces have been shown to give rise to photoluminescence bands specific to hydroxylated MgO. However, the mechanism responsible for the photoluminescence of surface OH groups, as well as the assignment of the different species to local structures raise some problems.

The first one concerns the origin of the observed phenomena: Are the bands due to intrinsic luminescence of OH groups? The presence of quite similar photoluminescence emission signals in the 400−420 nm range described for various systems containing OH groups, either in solution[40] or on the surface of solids,[41−46] could suggest that an intrinsic luminescence of OH groups is involved. Merkel et Hamill[40] finally rejected this hypothesis because of the dependence of the intensity of the band on the amount of metallic impurities contained in solutions and alternatively proposed that this photoluminescence might involve "electron transfer in M−OH metal-hydroxide complexes". In the case of hydroxylated MgO surfaces, one could

SCHEME 2: Thermal Stability Ranges of the Luminescent Species Identified by the ($\lambda_{Exc}-\lambda_{Em}$) Couples, Observed on MgO after Adsorption of Water or Methanol

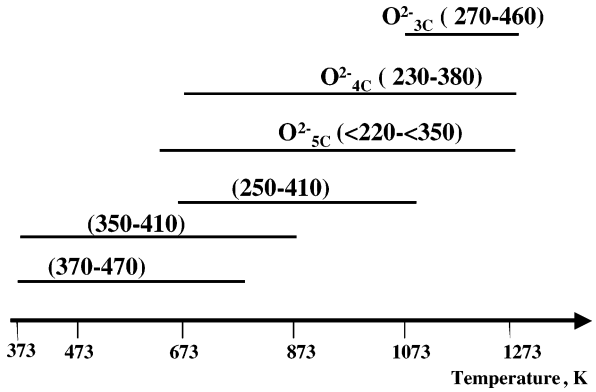

propose similarly that the photoluminescence is related to an electron transfer in the Mg−OH pair and the modification compared to the intrinsic MgO pair photoluminescence would be relative to the perturbation of energetic levels of MgO due to the presence of hydroxyls. However, taking into account that comparable emission bands are also observed in several OH containing systems,[40−46] we rather suggest a mechanism involving excitation of the Mg−OH pair followed by de-excitation via energy transfer to hydroxyl ions which then become the emitting sites. This mechanism is consistent with the fact that the excitation band positions are modified compared with those of the clean surface, and that only two broad emission bands are observed whereas there are at least three excitation sites.

The second problem concerns the assignment of the bands. Two questions can be raised: (i) Can hydroxyls formed from lattice oxygen, O_sH, or located on magnesium cations, O_wH (Scheme 1) be distinguished? (ii) By analogy with the case of the clean surface, is the assignment of the bands predominantly related to the coordination of the oxide ions or also influenced by lateral interactions involving hydrogen bonding, as usually considered in FTIR?[12,24]

Concerning the first question, it should be underlined that the luminescent species observed after water and methanol adsorption are the same. In the case of adsorption of methanol on ZnO, the enhancement of the emission intensity was assigned to molecularly adsorbed methanol and also to formation of methoxy species.[39] If adsorbed methanol and methoxy species can be evidenced on MgO by FTIR,[35] the formation of methoxy species is also accompanied by protonation of surface O^{2-} ions which gives rise to OH groups characterized by a FTIR band at 3740 cm^{-1}. Because the adsorption of water or methanol leads to the same three photoluminescent species (Table 3 and Figures 6 and 7), the enhancement of emission species intensity is likely to be due to the formation of O_sH groups in line with Scheme 1. These results suggest that O_wH groups, where O_w is monocoordinated, i.e., bonded to only one Mg cation, have the same qualitative characteristics in terms of wavelengthh as O_sH groups and thus cannot be distinguished from the latter. Quantitative measurements are being performed to confirm this hypothesis.

Concerning the second question, the thermal stability ranges of the luminescent species produced upon adsorption of water or methanol, gathered on Scheme 2 and obtained by following the appearance-disappearance of the corresponding bands with increasing temperature, should be considered. Scheme 2 shows that both (370−470) and (350−410) species are less stable than

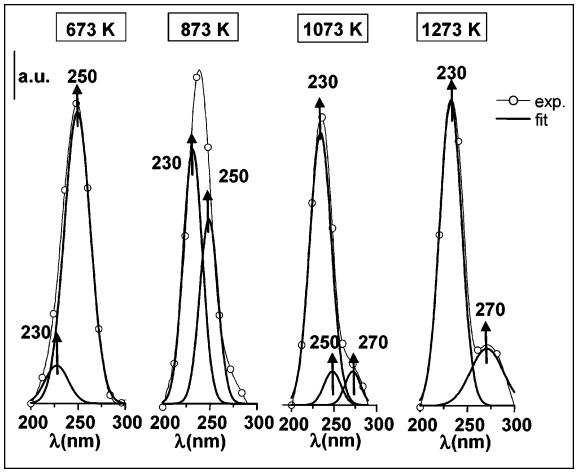

Figure 8. Decomposition of the excitation spectra of MgO−CVD treated under dynamic vacuum at 673, 873, 1073, and 1273 K.

(250−410) species as they are totally eliminated at 773 and 873 K, respectively. Note that surface OH groups involved in lateral interaction (IR band at 3600−3650 cm^{-1}) are also eliminated at 873 K (Figure 2). The (370−470) species reach their maximum of intensity before the (350−410) species (results not shown). The (250−410) species are more stable, and still observed at 873 K.

The spectra decompositions reported on Figure 8 evidence that the intensity of their bands decreases as soon as begins the recovering of bare $O^{2-}{}_{4C}$ ions at 673 K. The $O^{2-}{}_{3C}$ ions start to be recovered at higher temperature, 1073 K, when (250−410) species have almost disappeared. These results indicate that hydroxyls corresponding to protons covering both $O^{2-}{}_{4C}$ and $O^{2-}{}_{3C}$ are involved in the related bands and are thus at variance with Duley's interpretation obtained from the study of brucite dehydroxylation process or after subsequent rehydration.[45] Indeed, on the basis of the results of Henderson and Sibley,[44] Duley[45] considers that $O_{LC}H^-$ groups should respond in a manner similar to $O^{2-}{}_{LC}$. Hence, he proposed that the 470 nm emission feature is due to the hydroxyl group in a state of low coordination, $O_{LC}H^-$. This assignment is however inconsistent with the relative stability of the species (Scheme 2). The $O_{3C}H^-$ species are expected to be very stable,[47] as confirmed by our data with the recovering of $O^{2-}{}_{3C}$ from 1073 K, whereas the 470 nm emission disappears at lower outgassing temperature, 773 K. One can thus conclude that the coordination of oxide ions is not the only parameter to be considered in the assignment of the bands and that lateral interactions may be also involved.

Introduction of water (or methanol) on clean surfaces followed by outgassing at room temperature to remove gas phase in excess and physisorbed species first results in quenching of the signals of surface oxide ions, in relation with the remaining of surface chemisorbed water (or methanol). Moreover, the increase of the dissociation of water (or methanol) during the activation procedure, related to the progressive consumption of chemisorbed molecular water (or methanol) is another evidence for the presence molecular water on the surface during spectra recording. The presence of both molecularly adsorbed and dissociated species on MgO surface could be explained by a peculiar mechanism of water dissociation which is proposed, on the basis of theoretical and experimental studies on (100) MgO surfaces, to involve the participation of strongly adsorbed molecular water.[48−50] Even if there are not as many studies about methanol dissociation on MgO, FTIR characterizations[35−38] also evidence both dissociative and molecular adsorption for methanol at room temperature.

These features which are responsible for the apparent non selective disappearance of the photoluminesce of oxide ions imply that the first hydroxyl groups formed on MgO upon water or methanol dissociation are involved in lateral interaction.

From these results, and taking into account the relative thermal stability of the (350−410) and (370−470) species, we propose that both could be associated to an hydroxylated $Mg^{2+}{}_{LC}O^{2-}{}_{LC}$ surface, with hydroxyls groups involved in lateral interaction. The former one could be involved in hydrogen bonding with neighboring OH whereas the latter one could be involved in interaction with water (or methanol) molecules (Table 3).

The (250−410) species could be related to an hydroxylated $Mg^{2+}{}_{LC}O^{2-}{}_{LC}$ surface, with isolated hydroxyls groups, as represented in Table 3. Its stability range is consistent with that of the corresponding 3740 cm^{-1} IR band. Note that no interpretation can be proposed yet for the 310 nm excitation band observed in the case of MgO-sol−gel, due to its relative low intensity and to the ambiguous assignment of the corresponding emission band. Our assignment of (250−410) to the presence of isolated hydroxyls groups is consistent with that of Yoshida et al.[46] during the study of hydroxylation-dehydroxylation process of MgO supported on silica, Mg^{2+} ions being claimed to be dispersed as isolated monatomic species. The water introduction and spectrum recording procedures were quite comparable to ours. They also reported a shift to lower energy of the excitation when OH coverage was increased, indicating that the photoluminescence response depends on hydroxyl coverage of the surface, thus giving credit to the importance of lateral interactions in the assignment of the bands.

Conclusion

Discrimination of surface oxide ions with different coordination is greatly improved by means of in situ photoluminescence spectroscopy. The luminescence fingerprints ($\lambda_{exc}-\lambda_{em}$) of $O^{2-}{}_{5C}$, $O^{2-}{}_{4C}$, and $O^{2-}{}_{3C}$ correspond to (<220−<350), (230−380) and (270−460) couples, respectively. A pseudo quantitative evaluation of their distribution at MgO surfaces was obtained and shown to depend on the nature of the precursor (metallic magnesium or $Mg(OH)_2$ brucite phase) and on the morphology of the latter, in relation with the synthesis method. It should be underlined that the morphological characterization (TEM, XRD, BET) is consistent with molecular-level data (FTIR and in situ photoluminescence).

The photoluminescence response of hydroxylated MgO surfaces is also very specific, being sensitive to hydrogen bonding lateral interaction between OH groups and/or molecularly adsorbed water molecules. Excitation of the hydroxylated MgO surface leads to three bands (250, 350, and 370 nm) whereas deexcitation occurring via energy transfer to hydroxyls in Mg−O−H groups only gives two distinguishable contributions at 410 and 470 nm. It was shown from comparison of the relative stability of the three corresponding photoluminescent species that two of them are implied in hydrogen bonding and/or water interaction, whereas the thermally most stable one corresponds to isolated Mg−OH groups.

Study of the formation of photoluminescent Mg−OH groups upon introduction of water on bare surfaces evidences the presence of molecularly adsorbed water molecules. Consequently, because of the associated quenching phenomenon that unselectively leads to disappearance of all the oxide ions contributions, it is not possible, in case of water and methanol adsorption, to follow the preferential hydroxylation of the oxide ions of low coordination. However, the deprotonation of oxide

ions is selective: once the two contributions involved in lateral interactions have been eliminated by heating at 873 K, concomitantly with the decrease of the band associated with isolated OH, the O^{2-}_{4C} ions are recovered above 673 K, depending on the preparation of MgO, whereas O^{2-}_{3C} are liberated only above 10 73 K. Such results infer that O^{2-}_{3C} are more basic than O^{2-}_{4C} oxide ions.

The present work suggests that photoluminescence is one of the few techniques that allows the simultaneous study of oxide ions (versus their coordination number) and their corresponding protonated form: the $O^{2-}_{LC} \rightleftarrows OH^-$ transformation can be followed in situ as a function of temperature in the presence of protonated molecules. Photoluminescence appears thus as another interesting tool to evaluate the surface basic properties of oxides.

Acknowledgment. The authors wish to express their sincere gratitude to Pr. Erich Knözinger of the University of Wien and to Dr. Patricia Beaunier for kindly providing the MgO-CVD sample and the TEM micrographs, respectively.

References and Notes

(1) Hattori, H. *Stud. Surf. Sci. Catal*. **1985**, *21*, 319.
(2) Che, M.; Tench, A. J. *Adv. Catal.* **1982**, *31*, 77.
(3) Anpo, M.; Che, M. *Adv. Catal*. **1999**, *44*, 119.
(4) Tench, A. J.; Pott, G. T. *Chem. Phys. Lett.* **1974**, *26*, 590.
(5) Zecchina, A.; Lofthouse, M. G.; Stone, F. S. *J. Chem. Soc., Faraday Trans. 1* **1975**, *71*, 1476.
(6) Zecchina, A.; Stone, F. S. *J. Chem. Soc., Faraday Trans. 1* **1976**, *72*, 2364.
(7) Zecchina, A.; Stone, F. S. *J. Chem. Soc., Faraday Trans. 1* **1978**, *74*, 2278.
(8) Levine, J. D.; Mark, P. *Phys. Rev.* **1966**, *144*, 451.
(9) Shluger, A. L.; Sushko, P. V.; Kantorovich, L. N. *Phys. Rev. B* **1999**, *59*, 2417.
(10) Bailly, M. L.; Costentin, G.; Krafft, J. M.; Che, M. *Catal. Lett*. **2004,** *92*, 101.
(11) Coluccia, S.; Marchese, L.; Lavagnino, S.; Anpo, M. *Spectrochim. Acta A* **1987**, *43*, 1573.
(12) Knözinger, E.; Jacob, K. H.; Singh, S.; Hofmann, P. *Surf. Sci*. **1993**, *290*, 388.
(13) Cavalleri, M.; Pelmenschikov, A.; Morosi, G.; Gamba, A.; Coluccia, S.; Martra, G. *Stud. Surf. Sci. Catal*. **2001**, *140*, 131.
(14) Ricci, D.; Di Valentin, C.; Pacchioni G.; Sushko, P. V.; Shluger, A. L.; Giamello, E. *J. Am. Chem. Soc.* **2003**, *125*, 738.
(15) Thorms, H.; Epple, M.; Viebrock, H.; Reller, A. *J. Mater. Chem.* **1995**, *5*, 589.
(16) Coluccia, S.; Tench, A. J.; Segall, R. L. *J. Chem. Soc., Faraday Trans. 1*, **1979**, *75*, 1769.
(17) Becker, A.; Benfer, S.; Hofmann, P.; Jacob, K. H.; Knözinger, E. *Ber. Bunsen-Ges. Phys. Chem.* **1995**, *99*, 1328.
(18) Knözinger, E.; Diwald, O.; Sterrer, M. *J. Mol. Catal. A* **2000**, *162*, 83.
(19) Moodie, A. F.; Warble, C. E. *J. Cryst. Growth* **1971**, *10*, 627.
(20) Coluccia, S.; Baricco, M.; Marchese, L.; Martra, G.; Zecchina *A. Spectrochimica Acta* **1993**, *49A*, 1289.
(21) Goodman, J. F. *Proc. R. Soc. London, Ser. A* **1958**, *247*, 346.
(22) Gordon, R. S.; Kingery, W. D. *J. Am. Ceram. Soc*. **1966**, *49*, 654.
(23) Philippe, R.; Fujimoto, K. *J. Phys. Chem.* **1992**, *96*, 9035.
(24) Anderson, P. J.; Horlock, R. F.; Oliver, J. F. *Trans. Faraday Soc*. **1965**, *61*, 2754.
(25) Garrone, E.; Zecchina, A.; Stone, F. S. *Philos. Mag*. **1980**, *B42*, 683.
(26) Duley, W. W. *Philos. Mag*. **1984**, *B49*, 159
(27) Shvets, V. A.; Kuznetsov, A. V.; Fenin, V. A.; Kazansky, V. B. *J. Chem. Soc., Faraday Trans. 1*, **1985**, *81*, 2913.
(28) Anpo, M.; Yamada, Y.; Kubokawa, Y.; Coluccia, S.; Zecchina, A.; Che, M. *J. Chem. Soc., Faraday Trans. 1* **1988**, *84*, 751.
(29) Turro, N. J. *Molecular Photochemistry*; Benjamin: New York, 1967.
(30) Turro, N. J. *Modern Molecular Photochemistry;* Benjamin/Cummings: Menlo Park, CA, 1978.
(31) S. Coluccia, S.; Deane A. M.; Tench, A. J. *J. Chem. Soc., Faraday Trans. 1* **1978**, *74*, 2913.
(32) Coluccia, S.; Deane, M.; Tench, A. *J. Proceed. 6th. ICC, ed: The Chemical Society* **1977**, *1*, 171.
(33) Bailly, M. L.; Chizallet, C.; Costentin, G.; Lauron-Pernot, H.; Krafft, J. M.; Che, M., to be published
(34) Anpo, M.; Yamada, Y. *Mater. Chem. Phys.* **1988**, *18*, 445.
(35) Bensitel, M.; Saur, O.; Lavalley, J. C. *Mater. Chem. Phys.* **1991**, *28*, 309.
(36) Chauvin, C.; Saussey, J.; Lavalley, J. C.; Idriss, H.; Hindermann, J.; Kiennemann, A.; Chaumette, P.; Courty, P. *J. Catal*. **1990**, *121*, 56.
(37) Busca, G.; Lorenzelli, V. *Mater. Chem*. **1982**, *7*, 89.
(38) Spitz, R. N.; Barton, J. E.; Barteau, M. A.; Staley, R. H.; Sleight, A. W. *J. Phys. Chem.* **1986**, *90*, 4067.
(39) Idriss, H.; Barteau, M. A. *J. Phys. Chem.* **1992**, *96*, 3382.
(40) Merkel, P. B.; Hamill, W. H. *J. Chem. Phys.* **1971**, *55*, 2174.
(41) Tamura, H.; Rückschloss, M.; Wirschem, Th.; Veprek, S. *Appl. Phys. Lett.* **1995**, *65*, 1537.
(42) Rückschloss, M.; Wirschem, Th.; Tamura, H.; Ruhl, G.; Oswald, J.; Veprek, S. *J. Lumin.* **1995**, *63*, 279.
(43) Gimon-Kinsel, M. E.; Groothuis, K.; Balkus Jr. K. J. *Microp. Mesop. Mater.* **1998**, *20*, 67.
(44) Henderson, B.; Sibley, W. A.; *J. Chem. Phys.* **1971**, *55*, 1276.
(45) Duley, W. W. *J. Chem. Soc., Faraday Trans. 1* **1984**, *80*, 1173.
(46) Yoshida, H.; Tanaka, T.; Funabiki, T.; Yoshida, S, *J. Chem. Soc., Faraday Trans. 1* **1994**, *90*, 2107.
(47) Noguera, C. *J. Adhesion* **1996**, *57*, 91.
(48) Giordano, L.; Goniakowski, J.; Suzanne, J*; Phys. Rev. Lett*. **1998**, *81*, 1271.
(49) Kim, Y. D.; Lynden-Bell, R. M.; Alavi, A.; Stultz, J.; Goodman, D. W. *Chem. Phys. Lett.* **2002**, *352*, 318.
(50) Kim, Y. D.; Stultz, J.; Goodman, D. W. *J. Phys. Chem. B* **2002**, *106*, 1515.